arXiv:1210.6878v1 [quant-ph] 25 Oct 2012

Asymmetric Architecture for Heralded Single Photon Sources

Luca Mazzarella,[1,*] Francesco Ticozzi,[1,2,†] Alexander V. Sergienko,[3] Giuseppe Vallone,[1] and Paolo Villoresi[1]
[1]*Dipartimento di Ingegneria dell'Informazione, Università di Padova, via Gradenigo 6/B, 35131 Padova, Italy*
[2]*Department of Physics and Astronomy, Dartmouth College, 6127 Wilder Laboratory, Hanover, NH 03755, USA*
[3]*Department of Electrical and Computer Engineering,*
University of Boston, 8 Saint Mary's St., Boston, MA 02215, USA
(Dated: October 26, 2012)

Single photon sources represent a fundamental building block for optical implementations of quantum information. In this paper we propose a multiplexed system based on asymmetric configuration of multiple heralded single photon sources. The performance and the scalability comparison of the scheme to both existing multiple-source architectures and simple faint laser configuration reveals an advantage of the proposed scheme in realistic scenarios, and provide insights on the potential of these architectures for integrated implementation.

PACS numbers: 03.67.-a, 42.50.Gy, 42.50.Ex

I. INTRODUCTION

Single photon sources (SPSs) represent a key resource for optical quantum computing and communication. Indeed, optical quantum computers based on integrated photonic technology [1–4] can be build by using linear optics and SPSs as shown by Knill, Laflamme and Milburn [5]. On the other hand, current Quantum Key Distribution (QKD) systems [6–8] use weak laser pulses in place of single-photon sources and decoy state technique [9, 10] to avoid the photon splitting number (PNS) attack [11] on the pulses containing more than one photon. Using true single photon sources would guarantee that all pulses contain one and only one photon, increasing the key generation rate and avoiding any PNS attack.

The single photon source usually employed in quantum information applications is constituted by a faint laser (FL), namely an attenuated and pulsed laser source [23]. The number of photons in each pulse can be modeled, for a coherent source, by a Poisson random variable K with distribution:

$$\mathbb{P}(K=k)=\frac{\mu^k}{k!}e^{-\mu}, \tag{1}$$

where μ is the mean photon number in each pulse, which depends on the power of the laser. In order to evaluate the output quality of the source two indexes are usually employed: the *one-photon probability* $\mathbb{P}(K=1)$ and the *signal to noise ratio*:

$$\mathrm{SNR}:=\frac{\mathbb{P}(K=1)}{1-\mathbb{P}(K=0)-\mathbb{P}(K=1)}=\frac{\mu}{e^{\mu}-1-\mu}. \tag{2}$$

The SNR is the ratio between the one photon probability and the probability of having more than one photon in the output of the system. This index quantifies a critical quantity of the source: multiple photons per pulse, in fact, represent, in optical quantum computing, errors whose effects are hard to detect and correct, while, in QKD, they provide the possibility of PNS attacks.

The main limitations of the FL source stems from the fact that μ is the only tunable parameter. This induces a trade off: the value of μ that maximizes $\mathbb{P}(K=1)$ is given by $\mu=1$ and corresponds to a value of the one photon probability of $e^{-1}\simeq 0.37$. However, for $\mu=1$ the SNR is equal to $(e-2)^{-1}\simeq 1.39$, a value that is typically unacceptable for applications requiring a single photon source. Since the SNR is unbounded for μ approaching zero, the mean photon number is usually kept low in order to avoid multiple photons events, reducing also the probability of single photon emissions. To overcome the limitations of FL source, in the last years architectures with multiple heralded SPS have been proposed. Photons are generated by means of spontaneous parametric down conversion (SPDC): an intense laser pump impinging on a nonlinear crystal leads to probabilistic emission of entangled pairs of photons into two different spatial modes, with their rate depending on the pump intensity. It is then possible to "herald" the presence of a photon in one of the modes by detecting the correlated twin photon in the other one.

Post-selection schemes in combination with multiple heralded SPS have been first proposed by Migdall [12] in order to enhance the probability of obtaining a single heralded photon, with an implementation that requires an m-to-1 global switch. In the same work, the performance of the proposed scheme for finite detection efficiency were studied. However, as pointed out in [13], an efficient implementation of such device is not currently available, and it would be hardly scalable. To overcome these problems a symmetric scheme, employing a total of $m-1$ binary polarization-switching photon routers arranged in a modular tree structure has been proposed by Shapiro and Wong in [13], where they also evaluate the probability of emitting n photons taking into account imperfect detectors and optical switches. An experimental implementation of the scheme has been pursued in [14] using 4 crystals, along with an essential discussion of its

---

[*] Electronic address: mazzarella@dei.unipd.it
[†] Electronic address: ticozzi@dei.unipd.it

scalability. Recently, the analysis of multimode emission in SPDC used for SPS was carried out [15].

However, a thorough analysis of the performance of these sources in the presence of finite efficiencies, and their comparison with respect to a simple faint-laser source, is lacking: nonetheless, it appears to be a crucial step in assessing their potential, especially in the light of the experimental difficulties reported in [14]. In pursuing this analysis, we believe that one of the most delicate point consists in devising proper performance indexes, ensuring a fair comparisons between different methods.

In this paper, after reviewing the main ideas and theoretical result underlying the existing SPS architectures, we propose a new heralding scheme based on an asymmetric configuration. Next, we develop a comprehensive comparison between the architectures, that investigates the comparative performance, the scalability and the limits of SPS with multiple heralded sources in realistic scenarios.

II. REVIEW OF HERALDED SOURCES

A. Multiple sources and the advantage of post-selection

In this section we present the key ideas underlying a class of source architectures that outperform the FL scheme. The building block of such architectures is represented by the so-called Heralded Source (HS). The HS exploits the SPDC effect on a non-linear crystal pumped with a strong coherent field, which leads (with a certain probability) to the simultaneous generation of a pair (or more pairs) of photons. One photon of the pair is then fed to a photon detector: if the duration of the pulse (Δt_p) is much shorter than the measurement time interval (ΔT), but much greater than the reciprocal of the phase-matching bandwidth i.e., ($\Delta\omega$), i.e. $\Delta T >> \Delta t_p >> 1/\Delta\omega$, the statistics of the pairs is still Poissonian [13].

The HS can be employed in multiple crystal strategies that outperform the FL by exploiting the parallel use of HS units and post selection strategies: intuitively, the advantage of using a scheme exploiting a parallel implementation lies in the fact that the intensity of the pump of each crystal can be kept low, suppressing thus the multi-photons events, while keeping an acceptable production rate of single photons.

Let us assume for now to employ ideal detectors in order to illustrate in a simple setting the potential advantages offered by this system. The case of finite efficiency will be discussed later in this section.

We consider standard APD detectors: the information that these detectors provide is limited, since they are only able to discriminate between the case of no incident photons and the case in which photons are detected, without resolving their number. When a detector is hit by the photons, it returns an electric signal (*trigger*), which indicates the presence of at least a photon in the channel. A trigger event may be described by a Bernoulli random variable τ with values 0 or 1.

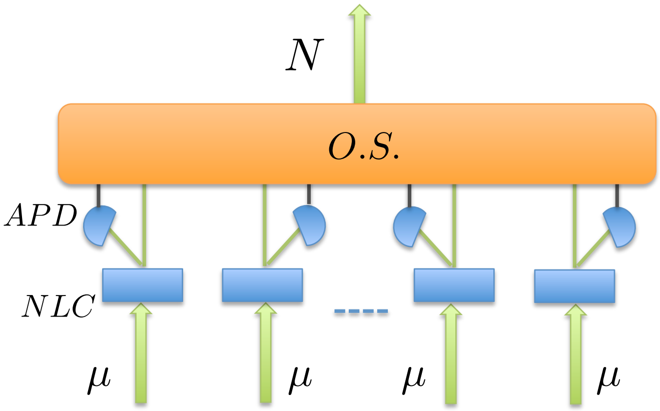

FIG. 1: Schematic of the MHPS scheme. The blue rectangles labeled with *NLC* represent the non-linear crystals, the detectors are labelled with *APD* and the orange rectangle, labelled with *O.S.*, represents the optical switch.

Let us consider a Multiple Crystals Heralded Source Architecture with Post-Selection (MHPS) built as follows: an array of m HS units, labelled with index $i = 1, \dots, m$, and each one simultaneously fed with a laser pulse with intensity such that the mean number of produced pairs is $\tilde{\mu}$. For each HS unit, one mode, corresponding to one of the photons in the SPDC pair, is used as trigger and the other is injected into an optical switch. Let τ_i and N_i be the trigger variable and the random variable (r.v.) accounting for the number of photons generated at the i-th source. We introduce a r.v. χ, called *post-selection function*, that is a deterministic function of $\tau_1, \dots, \tau_m$ such that:

$$\chi(\tau_1, \dots, \tau_m) \in \{0, 1, \dots, m\}. \tag{3}$$

The outcome of χ represents *the channel that we select to be routed to our global output*: this channel will correspond to the output of the i-th source when $\chi \in \{1, \dots, m\}$, otherwise, when $\chi = 0$, no channel will be selected. We then denote $\hat{N} = N_\chi$ as the r.v. accounting for the output statistics.

In other words, we assume to have an optical switch that is able to select one channel among the others according to the selection rule specified in (3). As first proposed in [12], we may assume:

$$\chi(\tau_1, \dots, \tau_m) = i \quad \text{with} \quad \tau_i = 1 \text{ and } \tau_{j<i} = 0\,. \tag{4}$$

Furthermore, we assume that if all the detectors do no fire:

$$\chi(\tau_1 = 0, \dots, \tau_m = 0) = 0. \tag{5}$$

This choice of the the χ function correspond to the following strategy: the output signal is taken from the first source (starting from $i = 1$) that triggers (thus indicating the presence of at least a photon in the channel). It is worth noting that the precise structure of χ is not important in this ideal situation. In fact, any selection function satisfying $\chi(\tau_1, \ldots, \tau_m) = i$ if at least $\tau_i = 1$ could be used in place of (4) without altering the performances. We will see in the next section how different selection rules affects crucially the performances once non-ideal situation are kept into account.

In order to derive the output statistics for the MHPS, let us first compute the probability that $\chi \neq 0$:

$$\mathbb{P}(\chi \neq 0) = 1 - \prod_{i \neq 0}^{m} \mathbb{P}(\tau_i = 0) = 1 - e^{-m\tilde{\mu}}\,, \tag{6}$$

as well as the probability of having n photons in the global output, given that $\chi = i$:

$$\mathbb{P}(\hat{N} = n | \chi = i) = \begin{cases} \frac{\frac{\tilde{\mu}^n}{n!} e^{-\tilde{\mu}}}{(1-e^{-\tilde{\mu}})}(1 - \delta_n), & \text{if } i \neq 0 \\ \delta_n, & \text{if } i = 0. \end{cases} \tag{7}$$

In the previous expression δ_n is the Kronecker Delta ($\delta_0 = 1$ and $\delta_{n \neq 0} = 0$). We thus have that the probability of having n photon in the global output of the MHPS is given by:

$$\begin{aligned} \mathbb{P}(\hat{N} = n) =& \mathbb{P}(\hat{N} = n | \chi \neq 0)\mathbb{P}(\chi \neq 0) + \\ &+ \mathbb{P}(\hat{N} = n | \chi = 0)\mathbb{P}(\chi = 0) \\ =& \frac{\tilde{\mu}^n}{n!} e^{-\tilde{\mu}} \frac{1 - e^{-m\tilde{\mu}}}{1 - e^{-\tilde{\mu}}}(1 - \delta_n) + \delta_n e^{-m\tilde{\mu}}. \end{aligned} \tag{8}$$

In particular, for the $\hat{N} = 1$ case:

$$\mathbb{P}(\hat{N} = 1) = \tilde{\mu} e^{-\tilde{\mu}} \frac{1 - e^{-m\tilde{\mu}}}{1 - e^{-\tilde{\mu}}}. \tag{9}$$

Let us now compare the performances of the MHPS with the performances of FL. Using (2) we find that the expression of the SNR for the MHPS is given by:

$$\text{SNR} := \frac{\tilde{\mu} e^{-\tilde{\mu}}}{1 - e^{-\tilde{\mu}} - \tilde{\mu} e^{-\tilde{\mu}}}. \tag{10}$$

Notice that, when $\tilde{\mu} = \mu$, the signal to noise ratio is equal to the SNR of the Faint Laser, while the single photon probability $\mathbb{P}(\hat{N} = 1)$ is always larger. In Table I we listed the one photon probability for different values of the SNR and of the number of crystals. The benefits of the MHPS with respect to the FL are apparent: fixed any SNR level, it is possible to obtain a higher value of the one photon probability. This is because of the post selection procedure, that can turn (with a certain probability) events in which more than one detectors trigger at the same time into an event that corresponds to a one-photon output *by blocking the output of all the HS units but one.*

TABLE I: One photon probability for the FL and the MHPS scheme, with $m = 4, 8$ and 16.

	$\mathbb{P}(\hat{N} = 1)$			
SNR	FL	MHPS-4	MHPS-8	MHPS-16
10	0.156	0.480	0.707	0.864
20	0.088	0.306	0.513	0.750
50	0.038	0.143	0.265	0.456

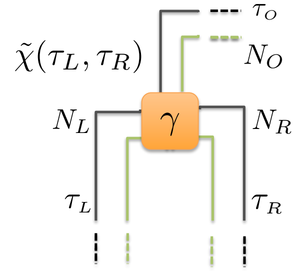

FIG. 2: Schematic of the binary switch.

Before closing this section we consider the ideal performances of the MHPS performances in the limit of an infinite number of crystals. In this case, in order to avoid the need of infinite pump power, we must rescale the intensity as $\mu \to \mu/m$. This is equivalent of using a parallel strategy in which a single laser beam of intensities μ is split into m beams with intensity $\tilde{\mu} = \mu/m$ shining m different crystals. In the infinite number of crystal limit we get:

$$\lim_{m\to\infty} \mathbb{P}(\hat{N} = 1) = 1 - e^{-\mu}. \tag{11}$$

This expression can be rewritten as $1 - (e^{-\frac{\mu}{m}})^m$, representing the complement of the probability of not having triggers among all the detectors, i.e, the probability that at least one among them triggers. This means that, since we are using an infinite number of crystals, the intensity per single crystal goes to zero, and so does the probability of generating multiple photons in a single crystal: each crystal is going to produce either one or no pairs. This also implies that the MHPS achieves an infinite value for the SNR as can be easily seen from (10).

B. Finite efficiency and symmetric modular architecture

Any discussion regarding the physical implementations would be vain without taking into account the realistic efficiencies in detection and routing of the produced photons. An actual detector, in fact, is subject to losses whose effects are usually described by introducing a parameter $0 \leq \eta \leq 1$, called *detection efficiency*, that represents the probability of detection of an incident photon. This parameter takes into account also the collection efficiency, as the phase matching relations yield uncertainty

τ_L	τ_R	$\tilde{\chi}(\tau_L, \tau_R)$
0	0	0
0	1	R
1	0	L
1	1	L

TABLE II: Definition of the selection function $\tilde{\chi}$

in the direction of the emitted photons.

Physical implementation of post-selection rules are subject to losses as well. The efficiency in transmission is modeled with a parameter $0 \leq \gamma \leq 1$, called *transmissivity*, that represents the probability of transmission for a photon through the router. It is important to note that this limited efficiency is referred only to the transmission of the photons: for what it concerns the transmission of the electrical signal we are always going to assume that, once a trigger happen, it is transmitted until the end of the transmission chain without errors.

We remark that, in order to consider the role of a finite transmissivity, it is key to specify the particular routing/switching architecture that is being considered, since the potential gain with respect to a FL (without the routing inefficiencies) will in general depend on it. This is not the case in the ideal scheme described in the previous section: expressions (8) and (10) do not depend on the particular χ chosen as long as it satisfies (4) and (5).

In what follows we are going to briefly review a modular architecture, proposed in [13], that employs binary photon routers (2-to-1) whose working mechanism is depicted in fig. 2: $\tau_{R,L} \in \{0, 1\}$ are Bernoulli r.v. accounting for the trigger signal incoming from the previous level. We introduce the r.v. $\tilde{\chi}$, called selection function, that is a deterministic function of τ_L and τ_R as defined in table II. Therefore, $\tilde{\chi}$ accounts for which channel is driven through the router.

The m-HS units are arranged as shown in fig. 3, where τ_i, with $i = 1, \dots, m$, are r.v. accounting for the trigger of the i-th channel. The outputs of the first stage are fed into the second stage's routers and so on, until the end of the transmission chain. This architecture can be clearly realized only for $m = 2^k$, with $k \in \mathbb{N}$.

It is worth noting that any successfully transmitted photons have to pass trough $k = \log_2 m$ routers. We will call this scheme Symmetric Multiple-crystals Heralded-Source with Post-selection (SMHPS). The overall effect of the selection function implemented in the routers is that, if more than one detectors fire, the channel routed to the end of the chain is the one coming from the crystal corresponding to the lowest i. More precisely, this architecture is efficiently implementing the post-selection function χ given in (4).

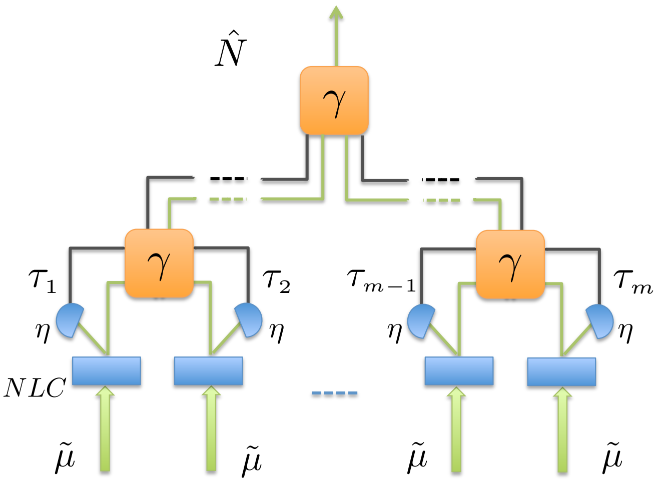

FIG. 3: Schematic of the SMHPS scheme proposed in [13]. The blue rectangles labeled with NLC represent the non-linear crystals, the detectors are labelled with η and the orange squares, labelled with γ, are the photon routers.

The corresponding probability of having n photons in the final output can now be computed to be:

$$\mathbb{P}(\hat{N} = n) = e^{-\eta 2^k \tilde{\mu}} \delta_n + \frac{\left(\tilde{\mu}\gamma^k\right)^n e^{-\tilde{\mu}\gamma^k}}{n!} \frac{1 - (1-\eta)^n e^{-\eta(1-\gamma^k)\tilde{\mu}}}{1 - e^{-\eta\tilde{\mu}}} (1 - e^{-\eta 2^k \tilde{\mu}}) \tag{12}$$

The first term in the previous sum account for the probability of having no photons in the output because no detector fired. We will postpone the performances comparison of SMHPS with the FL in section III.

III. ASYMMETRIC ARCHITECTURE

A. Analysis of the 2-crystal architecture: Symmetry is not optimal

In the all the previous works, it was assumed that all the crystals were driven with same intensity. We will now prove that this choice represents a suboptimal case for the one photon probability.

In order to do so, let us derive the probability of having one photon in the output of a MHPS composed by two crystals each one be fed with different intensities such that the mean number of emitted pairs is μ_j. Let us call $\hat{N}$ the r.v. accounting for the statistics of the final output while N_1 (N_2) and τ_1 (τ_2) accounts for the statistics and trigger of the first (second) channel respectively. Let χ be a post-selection function as specified in the previous section.

The probability that the first and the second detector give rise to a trigger is given respectively by:

$$\mathbb{P}(\chi = 1) = (1 - e^{-\mu_1}), \tag{13}$$

$$\mathbb{P}(\chi = 2) = (1 - e^{-\mu_2}) e^{-\mu_1}. \tag{14}$$

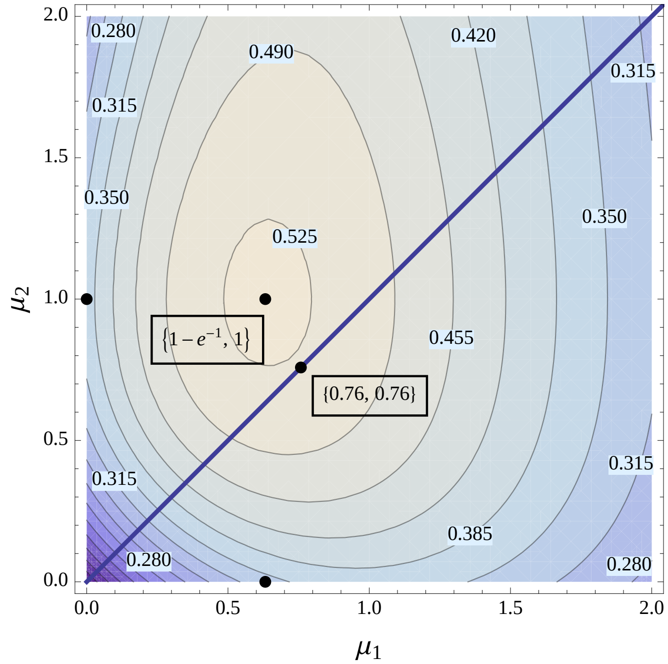

FIG. 4: Contours of the one-photon probability (15) for the two crystals MHPS. The blue line represent the $\mu_1 = \mu_2$ case.

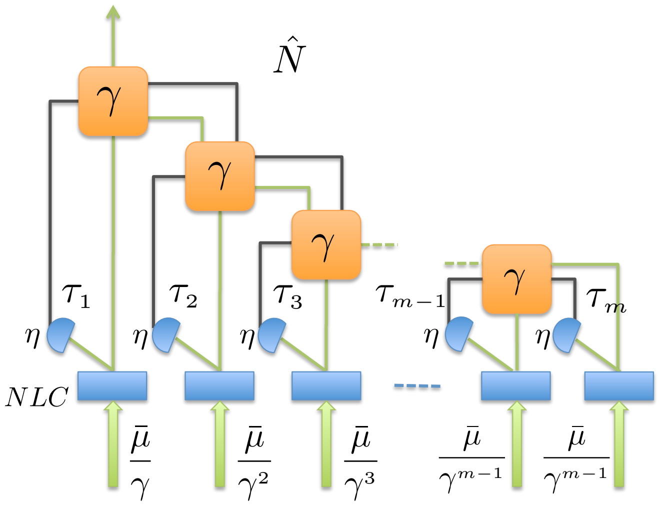
$\hat{N}$
γ
γ
γ
γ
τ_1
τ_2
τ_3
τ_{m-1}
τ_m
η
η
η
η
η
NLC
$\frac{\bar{\mu}}{\gamma}$
$\frac{\bar{\mu}}{\gamma^2}$
$\frac{\bar{\mu}}{\gamma^3}$
$\frac{\bar{\mu}}{\gamma^{m-1}}$
$\frac{\bar{\mu}}{\gamma^{m-1}}$

FIG. 5: Schematics of the AMHPS. Notice that each crystal is fed with different intensities to compensate the different absorption rate of different channels.The blue rectangles labeled with NLC represent the non-linear crystals, the detectors are labelled with η and the orange squares, labelled with γ, are the photon routers.

while the probability of having one photon in the final output is given by:

$$\mathbb{P}(\hat{N} = 1) = \mu_1 e^{-\mu_1} + \mu_2 e^{-(\mu_1+\mu_2)}. \tag{15}$$

The maximum of $\mathbb{P}(\hat{N} = 1)$ is achieved when

$$(\mu_1, \mu_2) = (1 - e^{-1}, 1). \tag{16}$$

This can be seen in fig. 4 where the contours of $\mathbb{P}(\hat{N} = 1)$ are plotted: the blue line represent the cases $\mu_2 = \mu_1$.

Therefore, we conclude that, in general, feeding all the crystals with the same laser intensities, leads to suboptimal performances. It is worth noticing that the asymmetry comes from the selection function $\tilde{\chi}$ of Table 3, where the first source is initially checked and, only if this source doesn't trigger, the selection function consider the second source. As we demonstrated, this asymmetry can be exploited to improve the probability of having one photon at the output channel.

In the ideal case (perfect detection and transmission), it is straightforward to compute the intensities that lead to the one photon probability optimal value generalizing the analysis above. Anyway, such optimization task become quite non-trivial if finite efficiency are taken into account, especially for a large number of crystals.

B. Proposed asymmetric architecture

Here we would like to propose an alternative (still suboptimal) scheme which can be realized with an arbitrary number of crystals and achieves better performances than the SMHPS in many situation of experimental interest.

Let us again suppose to have an array of m-HS system. Let τ_i and N_i be the r.v. accounting for the trigger and the number of photons in the input of the i-th channel respectively. Finally μ_i is the mean number of generated pair of the i-th crystal. This new scheme also employes binary switches but the multiplexing is performed in a different way, as displayed in fig. 5: the m-th source is multiplexed with the (m-1)-th, the output is then multiplexed with the (m-2)-th source, and so on. In this new configuration each successfully transmitted photon passes through a number of photon routers k_i that depends on which crystal it has been created from. More precisely, it is given by:

$$k_i = \begin{cases} i, & \text{if } \ i \leqslant m-1 \\ m-1, & \text{if } \ i = m. \end{cases} \tag{17}$$

Since each channel is subjected to a different attenuation (see (17)), we compensate the different absorption rates by choosing the input intensities as follows:

$$\mu_i = \frac{\bar{\mu}}{\gamma^{k_i}}\,, \qquad i = 1, \ldots, m. \tag{18}$$

This choice is still suboptimal but is sufficient to outperform the SMHPS in many situation of experimental interest.

This multiplexing architecture is therefore asymmetric and will be denoted with AMHPS, to highlight the differences with the SMHPS scheme. It is worth to note that both the symmetric than the asymmetric architecture require the same number of detectors and routers. With each binary switch configured as before, the channel that we select to be routed to our global output, is here determined by:

$$\chi = \begin{cases} i, & \text{if } \tau_i = 1 \text{ and } \tau_j = 0 \text{ for } j = 1, \dots, i-1, \\ 0 & \text{if } \tau_j = 0 \text{ for } j = 1, \dots, m. \end{cases} \tag{19}$$

It is worth noting that, the global effect of this rule, within this architecture, is that if two or more channels are heralded, the one that needs to pass through less routers is selected and routed to the end of the chain, thereby decreasing the probability of absorption.

As shown in appendix A, the probability of emitting n-photons for the AMHPS is given by:

$$\begin{aligned} \mathbb{P}(\hat{N} = n) &= \delta_n e^{-\eta\bar{\mu}\frac{(2-\gamma)\gamma^{1-m}-1}{1-\gamma}} + \\ &+ \frac{\bar{\mu}^n e^{-\bar{\mu}}}{n!} \sum_{i=1}^{m} e^{-\eta\bar{\mu}\frac{\gamma^{1-i}-1}{1-\gamma}} \left[1 - (1-\eta)^n e^{\eta\bar{\mu}} e^{-\frac{\eta\bar{\mu}}{\gamma^{k_i}}}\right]. \end{aligned} \tag{20}$$

It worth noting that, by using the compensation proposed in (18), the dependence of the one photon probability on the intensities is reduced to a single variable, i.e. $\bar{\mu}$. Moreover, when $\gamma \to 1$, the value of $\mathbb{P}(\hat{N} = n)$ for the asymmetric scheme coincide with the values (12) of the symmetric scheme for any value of η.

In the next section we are going to confront the FL, the SMHPS and the AMHPS with the compensation we have proposed.

IV. PERFORMANCE COMPARISON

A. Maximum probability with guaranteed SNR

This section is devoted to the comparison of the FL, the SMHPS and the AMHPS by means of numerical considerations. As we have stated previously, in many application it is crucial to be able to rely on a threshold value for the SNR. With this in mind, we propose the following method for the comparison: we fix a threshold value for the acceptable SNR, Θ, and for each architecture, given pair of efficiencies (η, γ) and for a given number of crystals, we compute the optimal pump intensity for which:

$$\bar{\mu}(\eta, \gamma, \Theta) = \arg \max_{SNR \geqslant \Theta} \mathbb{P}(\hat{N} = 1, \mu, \eta, \gamma), \tag{21}$$

i.e., we compute the intensity that maximize the one photon probability provided that the SNR has a greater or equal value than Θ. We notice that, since $\lim_{\mu \to 0} \text{SNR} = +\infty$ and $\lim_{\mu \to +\infty} \text{SNR} = 0$ for both the symmetric than the asymmetric scheme, by choosing the appropriate value of μ, any value of the SNR can be achieved.

We finally compare the one photon probability for different methods constrained to the optimal intensities:

$$\overline{\mathbb{P}}(\hat{N} = 1) = \mathbb{P}(\hat{N} = 1, \bar{\mu}(\eta, \gamma, \Theta), \eta, \gamma). \tag{22}$$

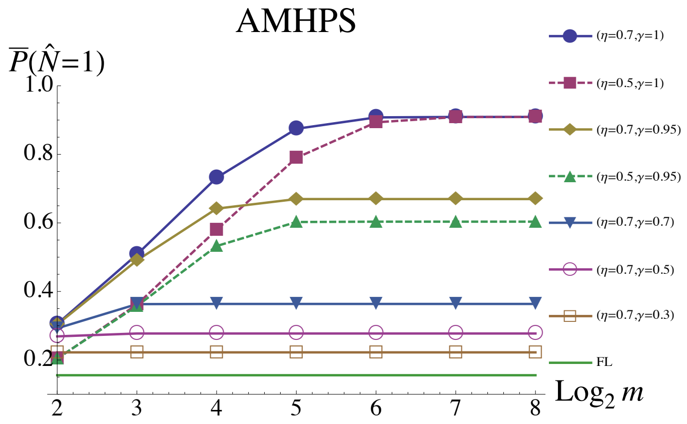

FIG. 6: One-photon probability for the AMHPS with $\Theta = 10$ and $m \in \{4, \dots, 256\}$ and various pairs of (η, γ).

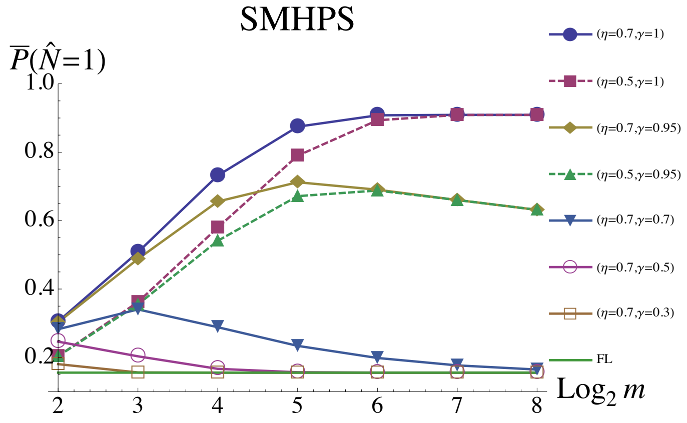

FIG. 7: One-photon probability for the SMHPS with $\Theta = 10$ and $m \in \{4, \dots, 256\}$ and various pairs of (η, γ).

Notice that, once the number of crystals and the SNR threshold are fixed, the above quantity depends only on (η, γ). From now on, $\overline{\mathbb{P}}(\hat{N} = 1)$ always indicates this optimized probability with the SNR constraint.

B. Scalability of the schemes for finite efficiencies

We first discuss the scalability features of the strategies with respect to the total number of crystals. In fig. 6-7 we plotted the values of $\overline{\mathbb{P}}_A(\hat{N} = 1)$ and $\overline{\mathbb{P}}_S(\hat{N} = 1)$ versus the number of crystals, m, ranging from 4 to 256 for different pairs of (η, γ) and for threshold SNR given by $\Theta = 10$.

For what concern the AMHPS it is apparent that, for all the considered pairs of (η, γ), the one photon probability increases until it reaches an asymptotic value (the dependance of this value on γ and η is non-trivial). This fact implies that, once the detection efficiency and the transmissivity are fixed, there is a threshold value on the number of crystals above which there is no further improvement in the performances of the scheme. It is worth noting that for experimental realistic parameters, i.e. $\gamma \lesssim 0.5$, the asymptotic performances are practically already reached for $m = 8$.

For what it concerns the SMHPS, after an initial transient, the one photon probability starts to decrease (a part for the ideal case of $\gamma = 1$). We have analytically shown that, excluding the $\gamma = 1$ case, in the limit of infinite number of crystals ($m \to +\infty$) the one photon probability of the symmetric scheme approach the one photon probability of the faint laser when the pump parameters are chosen in order to have asymptotically the same SNR (as can be sees in fig. 7). The result is demonstrated in appendix C.

Let us try to give a motivation for this counter intuitive behavior: has we have mention above, in the SMHPS each successfully transmitted photon have to pass through $\log_2 m$ routers, increase the number of crystal means also to increase the absorption rate the photons are subjected to. Thus for this geometry architecture the benefits deriving from the increase of the number of crystals do not compensate the increase in the absorption rate. On the contrary, as we have mention above, in the AMHPS are most likely to be selected those channels whose photons have to pass through less routers in order to reach the global output leading, on average, to a lower absorption rate.

Summarizing, there are some benefits for the SMHPS in increasing the number of crystals but only up to a certain number, depending on the detection efficiency and transmissivity. Anyway increasing further the number of crystals will lead to poorer and poorer performances.

The AMHPS offers significant benefits in increase the number of crystal until a certain number depending on the detection efficiency and transmissivity, once the threshold is reached increasing further the number of crystal will left the performances unchanged. Finally, we remark that since the two methods employ the same post-selection rules, the gap in the performances arises form the different architecture geometries that is responsible for the different distribution of the routers.

Before closing this section, let us briefly review and discuss the scalability analysis proposed in [12]. In that paper, in order to evaluate the advantages of a scheme with respect to the FL, the *gain*, namely the ratio G between the one-photon probability of having one photon in the output of the SMHPS and the probability of producing one photon with the FL, is considered. It is worth remarking that in [12] the one-photon probability for the proposed scheme is computed neglecting both detection and transmission inefficiencies: in this ideal case, it turns out that both the scheme and the FL have the same SNR provided that the intensity with which the HS units are fed is equal to the intensity of the FL. In order to analyze the scalability taking into account the absorption due to the routing chain, they propose to consider the asymptotic behavior of the product $\gamma^k G$, thus comparing the benefits of a growing multi-crystal architecture to the increase in the absorption rate due to the longer routing chain. As a result of this analysis, we have that the advantage of the SMHPS is maintained (i.e. $\lim_{k\to\infty} \gamma^k G > 1$) if $\gamma \geq 1/2$.

In order to perform a similar analysis we should compare the asymptotic behavior, in the limit of an infinite number of crystals, of the rate between the one-photon probability for the SMHPS, (12), with the probability of producing one photon with the FL, for the same SNR. As shown in appendix C, in the $k \to \infty$ limit the SNR of the faint laser with intensity μ is equal to the SNR of the SMHPS with $\tilde{\mu} = \frac{\mu}{\gamma^k}$ (the number of crystal is $m = 2^k$). Moreover, as explained previously, in order to avoid infinite power we need to rescale the pump power (for both the FL than the SMHPS) with the number of crystal, $\mu \to \mu/2^k$. The gain we obtain is given by:

$$\widetilde{G} = \frac{(1 - e^{-\gamma^{-k}\eta\mu})[1 + e^{(-1+\gamma^k)\frac{\eta\mu}{(2\gamma)^k}}(\eta - 1)]}{1 - e^{-\frac{\eta\mu}{(2\gamma)^k}}} \tag{23}$$

In the infinite k limit, the gain $\widetilde{G}$ is greater than 1 for $\gamma \geq \frac{1}{2}$ (and is actually divergent for $\gamma > 1/2$) as found in [12]. However, in the rescaled pump power case, the one-photon probability of the SMHPS tends asymptotically to zero and the gain does not seems the proper index to evaluate the absolute performance of a scheme. In fact, despite exhibiting an advantage with respect to the FL, $\mathbb{P}(\hat{N} = 1)$ is asymptotically zero in both cases (as already said, without the rescaling $\mu \to \mu/2^k$, the single photon probability of the SMHPS and of the FL coincide in the large k limit, and the gain is always 1). This means that, with finite transmissivity, not only increasing the number of crystal beyond a certain value does not bring any advantage, but it is actually detrimental to the SMHPS scheme performance. On the other hand, the AMHPS scheme is "robust" with respect to implementations with large numbers of crystals, as it is clearly shown in fig. 6.

C. Comparison between AMHPS and SMHPS

In figures 8 and 9 we displayed the contours plot of $\bar{\mathbb{P}}(\hat{N} = 1)$ for the AMHPS and the SMHPS with SNR threshold given by $\Theta = 10$ and $m = 4$ and 8 respectively. The white zones correspond to the case in which $\bar{\mathbb{P}}(\hat{N} = 1)$ is below the value of the one-photon probability of the FL corresponding to an SNR equal to 10 (for the faint laser, when SNR=10 the one photon probability is given by 0.155). We can see that both the AMHPS and the SMHPS outperform the FL in a vast region of the plane (η, γ), but such region is wider for the AMHPS. As expected, the best performances are reached for high values of both the detection efficiency and the transmissivity: furthermore in this limit the two methods are comparable since for $\eta \to 1$ and $\gamma \to 1$ they both tend to the ideal situation of the MHPS.

In the light of the numerical results, we can conclude that systems that exploit post-selection can indeed offer benefits with respect to the FL, for a wide set of

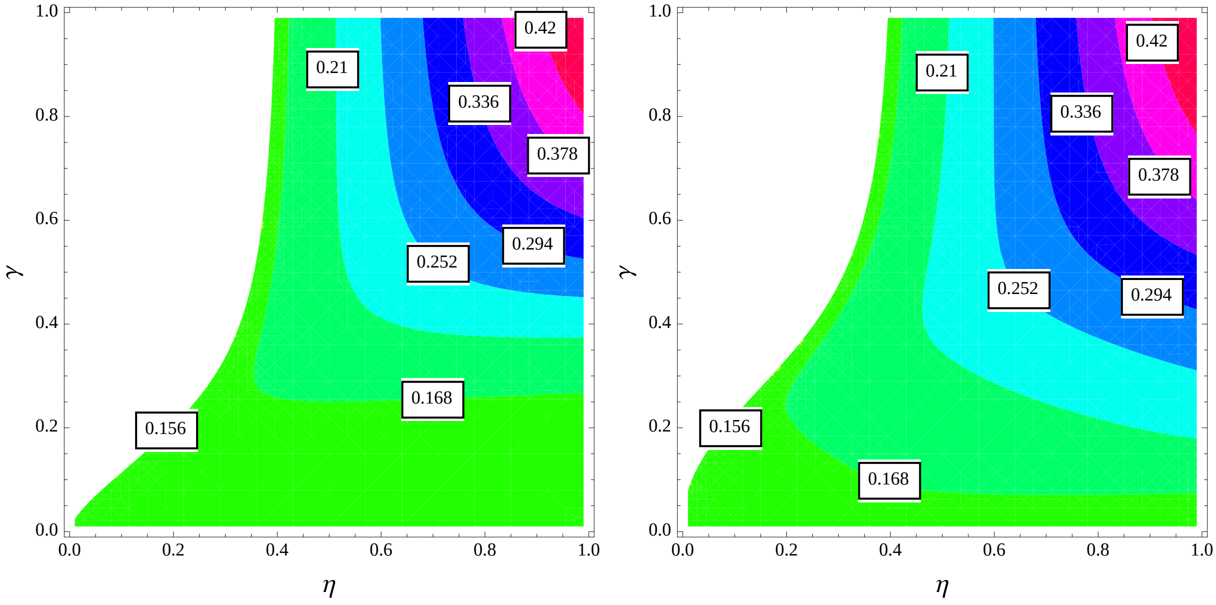

FIG. 8: Contours of the one-photon probability for the SMHPS (left) and the AMHPS (right) with guaranteed SNR, $\Theta = 10$, and $m = 4$. In the white area $\bar{\mathbb{P}}(\hat{N} = 1)$ is below the value of the one-photon probability (given by 0.155) of the FL with SNR equal to 10.

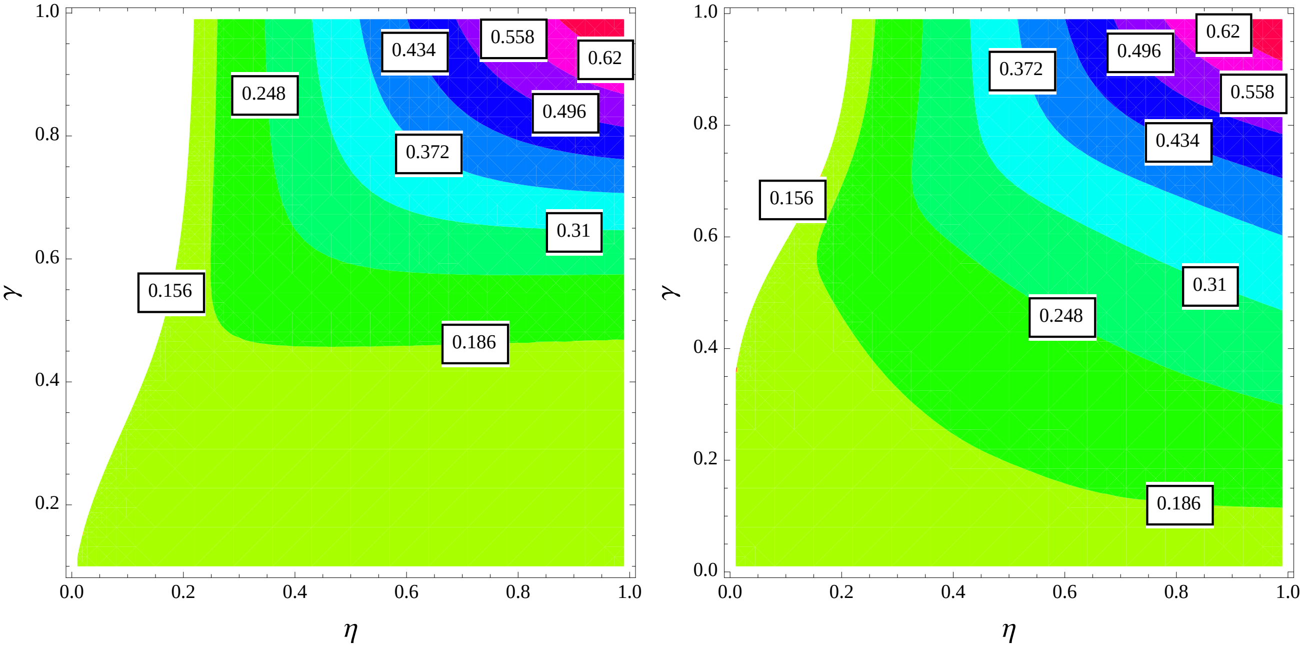

FIG. 9: Contours of the one-photon probability for the SMHPS (left) and the AMHPS (right) with guaranteed SNR, $\Theta = 10$, and $m = 8$. In the white area $\bar{\mathbb{P}}(\hat{N} = 1)$ is below the value of the one-photon probability of the FL with SNR equal to 10.

values of experimentally achievable detection efficiencies and transmissivities.

Let us now compare the AMHPS and the SMHPS. Let as call $\overline{\mathbb{P}}_A(\hat{N} = 1)$ and $\overline{\mathbb{P}}_S(\hat{N} = 1)$ the one-photon probability as computed in (22) for the AMHPS and the SMHPS respectively and let us define:

$$\Delta := \frac{\overline{\mathbb{P}}_A(\hat{N} = 1) - \overline{\mathbb{P}}_S(\hat{N} = 1)}{\overline{\mathbb{P}}_S(\hat{N} = 1)} \tag{24}$$

the percentage differences between the two single photon probabilities.

In fig. 10 and 11 we shown the contour of Δ for an

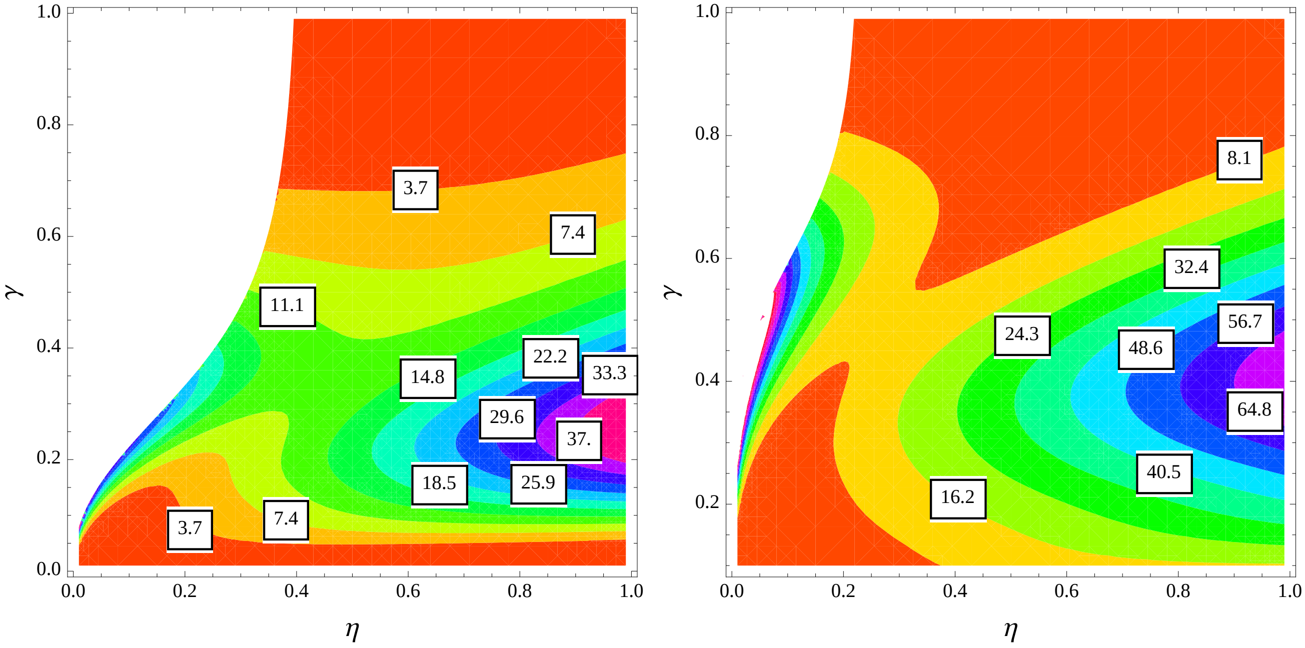

FIG. 10: Contours of the percentage differences (24) with guaranteed SNR, $\Theta = 10$, and $m = 4$ (left) or $m = 8$ (right). A positive number correspond to an advantage of the AMHPS to the SMHPS. In the white area $\bar{\mathbb{P}}_A(\hat{N} = 1)$ and $\bar{\mathbb{P}}_S(\hat{N} = 1)$ are both below the value of the one-photon probability of the FL with SNR equal to 10.

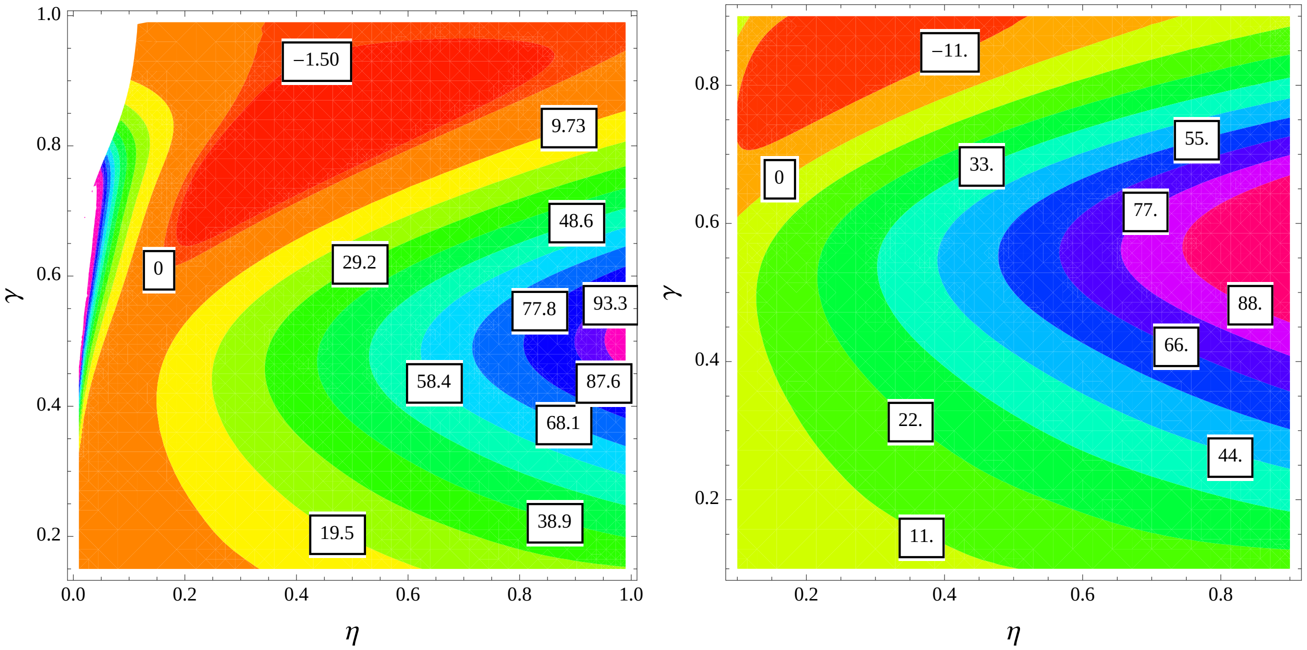

FIG. 11: Contours of the percentage differences (24) with guaranteed SNR, $\Theta = 10$, and $m = 16$ (left) or $m = 32$ (right). A positive number correspond to an advantage of the AMHPS to the SMHPS. In the white area $\bar{\mathbb{P}}_A(\hat{N} = 1)$ and $\bar{\mathbb{P}}_S(\hat{N} = 1)$ are both below the value of the one-photon probability of the FL with SNR equal to 10.

SNR equal to 10 and $m = 4, 8, 16$ and 32. The white zone are those in which neither $\bar{\mathbb{P}}_A(\hat{N} = 1)$ nor $\bar{\mathbb{P}}_S(\hat{N} = 1)$ are grater than the FL one-photon probability, that for and SNR of 10 is equal to 0.156.

In the case of $m = 4$ and $m = 8$ the AMHPS always outperforms the SMHPS. In the case of $m = 16$ and $m = 32$ the AMHPS outperforms the SMHPS in a vast portion of the plane (η, γ) even if a zone in which the SMHPS slightly outperforms (less than 2% for $m = 8$ crystals) the AMHPS is present for high value of γ. Anyway, the advantage of the AMHPS in more realistic situations is apparent, especially in the area where $\gamma \approx 0.5$ and the detection efficiency is higher than 0.5, the AMHPS significantly outperforms the SMHPS. Anyway, above $m = 32$ the AMHPS outperforms the SMHPS in every portion of the plane (η, γ) again.

V. EXPERIMENTAL FEASIBILITY AND CONCLUSIONS

Let us now discuss a possible experimental realization of the proposed SPS configuration. Nowadays, integrated devices represent the best resource to achieve high efficiency of the SPDC process and ensure good coupling into single mode fibers (for a review on integrated source see [16]). It is possible to use non-degenerate collinear phase matching and a dichroic beam splitter (or alternatively using a counterpropagating mode source [17]) in order to separate the two beams. For instance, it was recently reported the possibility of heralding single telecom photons at 4.4 MHz rate with 45% heralding efficiency [18]. Moreover, to efficiently detect the triggered photon, high efficient transition-edge sensors (TES) can be used: an heralding efficiency of $\eta \sim 62\%$ has been recently reported by using TES [19] (see also [20] for a review on single photon detectors). Regarding the optical switch, a 2x2 silicon electro-optic switches with a broad bandwidth (60 nm), an ultrafast speed (6 ns) and a transmission of $\gamma \sim 50\%$ has been reported [21]; other modulators otherwise allow lower losses at the cost of reduced working spectrum [22]. As shown in Fig. 8 with these values of η and γ the heralded schemes outperform the faint laser even with low number of crystal ($m = 4$), with the asymmetric scheme more performant than the symmetric one.

In conclusion we have proposed an asymmetric architecture for the multiplexed heralded single photon source and we have compared it with the symmetric version proposed in [13] and with the faint laser source. We have proven that the asymmetric architecture outperform the FL and the symmetric scheme in a vast region of the parameter space (η, γ). We have also demonstrated that, in the large number of crystal limit and by considering a fixed SNR, the symmetric configuration is asymptotically equivalent to the faint laser for any $\gamma \neq 1$, while for the asymmetric scheme the one photon probability increases until it reaches an asymptotic value dependent on γ and η. Values close to the asymptotic ones, at least for experimentally available efficiencies, are reached already around 8 crystals. This implies that, even if the expected energetic consumption for the AMHPS scheme is higher due to the implemented pre-compensation for the losses in the routing chain, the necessary overhead will be very limited. We believe that our results will be relevant to any future realization of heralded single photon source based on multiplexed architecture.

Acknowledgments

The Authors acknowledge the Strategic-Research-Project QUINTET of the Department of Information Engineering, University of Padova and the Strategic-Research-Project QUANTUMFUTURE of the University of Padova.

Appendix A: Statistics of the SMHPS

For the sake of completeness, let us provide a derivation for the SMHPS statistics presented in [13]. Given the post selection function χ of (4), the probability that $\chi = i$ is given by:

$$\begin{aligned}\mathbb{P}(\chi = i) &= \begin{cases}\mathbb{P}(\tau_i = 1)\prod_{l=1}^{i-1}\mathbb{P}(\tau_l = 0), & \text{if } i \neq 0,\\ \prod_{l=1}^{2^k}\mathbb{P}(\tau_l = 0) & \text{if } i = 0.\end{cases}\\ &= \begin{cases}(1 - e^{-\eta\tilde{\mu}})e^{-(i-1)\eta\tilde{\mu}}, & \text{if } i \neq 0,\\ e^{-\eta 2^k \tilde{\mu}} & \text{if } i = 0.\end{cases} \qquad \text{(A1)}\end{aligned}$$

The probability of having n photons in the i-th channel, given that $\chi = i$:

$$\mathbb{P}(N_i = j|\chi = i) = \begin{cases}\frac{\frac{\tilde{\mu}^j}{j!}e^{-\tilde{\mu}}(1-(1-\eta)^j)}{(1-e^{-\eta\tilde{\mu}})}, & \text{if } i \neq 0\\ \delta_j, & \text{if } i = 0.\end{cases} \qquad \text{(A2)}$$

The probability of having n photons in the final output given that $\chi = i$ and $N_i = j \geqslant n$ is given by:

$$\begin{aligned}&\mathbb{P}(\hat{N} = n|\chi = i, N_i = j) = \qquad \text{(A3)}\\ &= \begin{cases}\binom{j}{n}(\gamma^k)^n(1-\gamma^k)^{j-n}, & \text{if } i \neq 0 \text{ and } n \leqslant j\\ \delta_n, & \text{if } i = 0.\end{cases}\end{aligned}$$

Finally the probability of having n photons in the final output is given by:

$$\begin{aligned}\mathbb{P}(\hat{N} = n) =& \sum_{i=0}^{2^k}\sum_{j=n}^{\infty}\mathbb{P}(\hat{N} = n|\chi = i, N_i = j)\times \qquad \text{(A4)}\\ &\times \mathbb{P}(N_i = j|\chi = i)\mathbb{P}(\chi = i)\\ =&\delta_n e^{-\eta 2^k \tilde{\mu}} + \left[1 - (1-\eta)^n e^{-\eta(1-\gamma^k)\tilde{\mu}}\right]\times\\ &\times \sum_{i=1}^{2^k} e^{-(i-1)\eta\tilde{\mu}}\frac{(\tilde{\mu}\gamma^k)^n e^{-\tilde{\mu}\gamma^k}}{n!}.\end{aligned}$$

For which we have finally:

$$\begin{aligned}\mathbb{P}(\hat{N}=n) =& e^{-\eta 2^k\tilde{\mu}}\delta_n + (1-e^{-\eta 2^k\tilde{\mu}})\times \\ &\times \frac{\left(\tilde{\mu}\gamma^k\right)^n e^{-\tilde{\mu}\gamma^k}}{n!}\frac{1-(1-\eta)^n e^{-\eta(1-\gamma^k)\tilde{\mu}}}{1-e^{-\eta\tilde{\mu}}}\end{aligned} \tag{A5}$$

Appendix B: Statistics of the AMHPS

Here we explicitely derive eq. (20). Let $\hat{N}$ denote the r.v. accounting for the output statistics. The probability that a trigger coming from the i-th detector is routed to the global output is given by:

$$\begin{aligned}\mathbb{P}(\chi=i) &= \begin{cases}\mathbb{P}(\tau_i=1)\prod_{l=1}^{i-1}\mathbb{P}(\tau_l=0), & \text{if } i\neq 0,\\ \prod_{l=1}^{m}\mathbb{P}(\tau_l=0) & \text{if } i=0.\end{cases} \\ &= \begin{cases}(1-e^{-\eta\tilde{\mu}_i})\prod_{l=1}^{i-1}e^{-\eta\tilde{\mu}_l}, & \text{if } i\neq 0,\\ \prod_{l=1}^{m}e^{-\eta\tilde{\mu}_l} & \text{if } i=0.\end{cases}\end{aligned} \tag{B1}$$

The probability of having n photons in the i-th channel, given that $\chi=i$:

$$\mathbb{P}(N_i=j|\chi=i) = \begin{cases}\frac{\frac{\tilde{\mu}_i^j}{j!}e^{-\tilde{\mu}_i}(1-(1-\eta)^j)}{(1-e^{-\eta\tilde{\mu}_i})}, & \text{if } i\neq 0\\ \delta_j, & \text{if } i=0.\end{cases} \tag{B2}$$

The probability of having n photons in the final output given that $\chi=i$ and $N_i=j\geqslant n$ is given by:

$$\begin{aligned}&\mathbb{P}(\hat{N}=n|\chi=i,N_i=j) = \\ &= \begin{cases}\binom{j}{n}(\gamma^{k_i})^n(1-\gamma^{k_i})^{j-n}, & \text{if } i\neq 0 \text{ and } n\leqslant j\\ \delta_n, & \text{if } i=0.\end{cases}\end{aligned} \tag{B3}$$

It is worth noting that, the requirement that $n\leqslant j$ is due to the fact that the routing chain can only absorbs photons. Finally the probability of having n photons in the final output is given by:

$$\begin{aligned}\mathbb{P}(\hat{N}=n) =& \sum_{i=0}^{m}\sum_{j=n}^{\infty}\mathbb{P}(\hat{N}=n|\chi=i,N_i=j)\times \\ &\times\mathbb{P}(N_i=j|\chi=i)\mathbb{P}(\chi=i) \\ &= \delta_n\left(\prod_{l=1}^{m}e^{-\eta\tilde{\mu}_l}\right) + \sum_{i=1}^{m}\left(\prod_{l=1}^{i-1}e^{-\eta\tilde{\mu}_l}\right)\times \\ &\times\frac{(\tilde{\mu}_i\gamma^{k_i})^n e^{-\tilde{\mu}_i\gamma^{k_i}}}{n!}\left(1-(1-\eta)^n e^{-\eta(1-\gamma^{k_i})\tilde{\mu}_i}\right).\end{aligned} \tag{B4}$$

By computing the products we obtain (20).

Appendix C: Infinite crystals limit of the SMHPS

We here analytically show that the one photon probability of the symmetric scheme approaches the one photon probability of the faint laser when the pump intensities are chosen in order to have the same SNR. Let's consider the SHMPS with $\tilde{\mu}=\frac{\mu}{\gamma^k}$, where μ is the faint laser intensity and 2^k are the number of crystals. This is the natural choice in order to compensate the effect of the k routers that each emitted photon has to travel through. In this case the SNR of the SHMPS becomes

$$\frac{\mu\left[1-e^{-\frac{\eta\mu}{\gamma^k}}e^{\eta\mu}(1-\eta)\right]}{e^{\mu}-1-\mu-e^{-\frac{\eta\mu}{\gamma^k}}\left[e^{\mu}+e^{\eta\mu}(\eta\mu-\mu-1)\right]} \tag{C1}$$

In the large k limit, when $\gamma\neq 1$, the previous expression is equal to the SNR of the faint laser, namely $\frac{\mu}{e^{\mu}-1-\mu}$. For this choice of the pump parameter, namely $\tilde{\mu}=\frac{\mu}{\gamma^k}$, the SNRs are equal in the large k limit and the one photon probability of the SHMPS becomes

$$\begin{aligned}\mathbb{P}(\hat{N}=1) &= \frac{\mu e^{-\mu}[1-e^{-(\frac{2}{\gamma})^k\eta\mu}][1-e^{-\frac{\eta\mu}{\gamma^k}}e^{\eta\mu}(1-\eta)]}{1-e^{-\frac{\eta\mu}{\gamma^k}}} \\ &\sim \mu e^{-\mu} \quad \text{for } k\to\infty \text{ and } \gamma\neq 1\,,\end{aligned} \tag{C2}$$

asymptotic, in the large number of crystal limit, to the one photon probability of the faint laser.

---

[1] A. Politi, M. J. Cryan, J. G. Rarity, S. Yu, and J. L. O'Brien, Science **320**, 646 (2008).

[2] J. Matthews, A. Politi, A. Stefanov, and J. O'Brien, Nature Photonics **3**, 346 (2009).

[3] L. Sansoni, F. Sciarrino, G. Vallone, P. Mataloni, A. Crespi, R. Ramponi, and R. Osellame, Phys. Rev. Lett. **105**, 200503 (2010).

[4] A. Crespi, R. Ramponi, R. Osellame, L. Sansoni, I. Bongioanni, F. Sciarrino, G. Vallone, and P. Mataloni, Nature communications **2**, 566 (2011).

[5] E. Knill, R. Laflamme, and G. J. Milburn, Nature **409**, 46 (2001).

[6] V. Scarani *et al.* Rev. Mod. Phys. **81**, 1301 (2009).

[7] M. Canale, *et al.*, in Proceedings of the 4th International Symposium on Applied Sciences in Biomedical and Communication Technologies - ISABEL 2011, 1-5 (2011).

[8] D. Bacco *et al.*, in preparation.

[9] W.-Y. Hwang, Phys. Rev. Lett. **91**, 57901 (2003), ISSN 0031-9007.

[10] X. Ma, B. Qi, Y. Zhao, and H.-K. Lo, Phys. Rev. A **72**, 012326 (2005), ISSN 1050-2947.

[11] G. Brassard, N. Lütkenhaus, T. Mor, and B. Sanders, Phys. Rev. Lett. **85**, 1330 (2000), ISSN 0031-9007.

[12] A. L. Migdall, D. Branning, and S. Castelletto, Phys. Rev. A **66**, 053805 (2002).

[13] J. H. Shapiro and F. N. Wong, Opt. Lett. **32**, 2698 (2007).

[14] X.-s. Ma, S. Zotter, J. Kofler, T. Jennewein, and A. Zeilinger, Phys. Rev. A **83**, 043814 (2011).

[15] A. Christ and C. Silberhorn, Phys. Rev. L **85**, 1 (2012), ISSN 1050-2947.

[16] S. Tanzilli, A. Martin, F. Kaiser, M. De Micheli, O. Alibart, and D. Ostrowsky, Laser & Photonics Reviews **6**, 115 (2012), ISSN 18638880.

[17] X. Caillet, A. Orieux, A. Lemaître, P. Filloux, I. Favero, G. Leo, and S. Ducci, Optics Express **18**, 9967 (2010), ISSN 1094-4087.

[18] E. Pomarico, B. Sanguinetti, T. Guerreiro, R. Thew, H. Zbinden, "MHz rate and efficient synchronous heralding of single photons at telecom wavelengths", arXiv:1207.0441.

[19] D. H. Smith, G. Gillett, M. P. de Almeida, C. Branciard, A. Fedrizzi, T. J. Weinhold, A. Lita, B. Calkins, T. Gerrits, H. M. Wiseman, S. W. Nam, and A. G. White, Nat. Comm. **3**, 625 (2012), ISSN 2041-1723.

[20] M. D. Eisaman, J. Fan, A. Migdall, and S. V. Polyakov, Rev. Sci. Instrum. **82**, 071101 (2011), ISSN 00346748.

[21] P. Dong, S. Liao, H. Liang, R. Shafiiha, D. Feng, G. Li, X. Zheng, A. V. Krishnamoorthy, and M. Asghari, Optics Express **18**, 25225 (2010), ISSN 1094-4087.

[22] G. T. Reed, G. Mashanovich, F. Y. Gardes, and D. J. Thomson, Nature Photonics **4**, 518 (2010), ISSN 1749-4885.

[23] Employing driving fields allows for temporal localization of the photons and, in situation that require the use of detectors allow to avoid dark counts.